IOPscience iopscience.iop.org

Home Search Collections Journals About Contact us My IOPscience

The phase stability of the alkali-metal vanadates at high pressures studied by synchrotron X-ray powder diffraction and infrared spectroscopy

This article has been downloaded from IOPscience. Please scroll down to see the full text article.

1991 J. Phys.: Condens. Matter 3 6135

(http://iopscience.iop.org/0953-8984/3/32/018)

View the table of contents for this issue, or go to the journal homepage for more

Download details:
IP Address: 171.66.16.147
The article was downloaded on 11/05/2010 at 12:26

Please note that terms and conditions apply.

J. Phys.: Condens. Matter 3 (1991) 6135–6144. Printed in the UK

The phase stability of the alkali-metal vanadates at high pressures studied by synchrotron x-ray powder diffraction and infrared spectroscopy

David M Adams, Andrew G Christy, Julian Haines and Simon Leonard
Department of Chemistry, University of Leicester, Leicester LE1 7RH, UK

Received 12 December 1990, in final form 2 April 1991

Abstract. The materials AVO_3 (A ≡ K, Rb, Cs) have been studied at high pressure by energy-dispersive x-ray powder diffraction (EDXRPD) using synchrotron radiation. KVO_3 has also been investigated at high pressure by infrared spectroscopy.

$CsVO_3$ shows no phase change to 103 kbar. KVO_3 exhibits a sluggish phase change from 27 to 48 kbar. A structural model for the high-pressure phase is proposed, in which the vanadate chains slip relative to each other along their axes, generating a monoclinic cell (space group $P2/b11$, in a non-standard setting).

$RbVO_3$ shows a phase change at 40 kbar, indicated by a break in slope for plots of each of the lattice parameters against pressure. No other changes were evident in the EDXRPD pattern at this discontinuity. This is accounted for by a model in which the chains move relative to each other in the a-direction, maintaining the orthorhombic symmetry of the cell.

1. Introduction

There is a great variety of materials AMO_3 (where A is a mono- or divalent cation) in which there are chains of (MO_4) tetrahedra linked by common vertices. This is particularly true when M ≡ Si, but many examples are also known for M ≡ Ge, V and P. As part of a wider investigation of the phase stability of such materials, we report an x-ray powder diffraction and infrared study of the alkali-metal vanadates, AVO_3 (A ≡ K, Rb, Cs), under high applied pressures. The expectation was that these isostructural materials (*Pbcm*, $Z = 4$) [1] would behave analogously, showing phase transitions at cation-dependent pressures similarly to other alkali-metal salts, and yield useful compressibility data. What we have discovered confounds these expectations, and raises as many problems as it solves. The only previous high-pressure work on these materials is our own report on their vibrational spectra in which we observed a phase transition in $RbVO_3$ at 53 kbar, and found an indication of one in KVO_3 near 56 kbar [2].

2. Experimental procedure

The materials were those used earlier [2]. High-pressure EDXRPD data were obtained using samples in a gasketed diamond anvil cell (DAC) mounted in the synchrotron x-ray

0953-8984/91/326135+10$03.50 © 1991 IOP Publishing Ltd

beam at the SERC Daresbury Laboratory. Samples were contained within stainless steel (AISI 316) gaskets with a hole diameter of 300 μm, with methanol:ethanol as the quasi-hydrostatic pressure-transmitting medium. The incident x-ray beam was 100 μm in diameter. Pressures were estimated by the ruby fluorescence method. A relaxation time of about 1.5 h was allowed after each pressure change before x-ray measurement; exposure times were about 30 min.

Infrared spectra (4 cm^{-1} resolution) were acquired in a Bio-Rad Digilab FTS-40 spectrometer using the same DAC. KVO_3 was mixed with KBr and placed in the 400 mm gasket hole together with a layer of 0.21% w/w $NaNO_3$ in NaBr as pressure calibrant [3]. The sample temperature was 30 °C for all measurements.

3. Results

3.1. KVO_3

3.1.1. X-ray data. The EDXRPD data first showed new features at 27 kbar (see figure 1). These became increasingly prominent at higher pressures until, by 51 kbar, no sign remained of the parent orthorhombic phase. Thereafter, the diffraction pattern showed no change to a maximum pressure of 90 kbar.

The known orthorhombic cell was refined at atmospheric pressure using *d*-spacings from experiment. The results were in close agreement with those from the single-crystal report [1]. Plots of the refined lattice parameters to 50 kbar are seen in figure 2. Their pressure derivatives yield the uniaxial and volume compressibilities shown in table 1.

Table 1. Uniaxial ($\times 10^4$ kbar) and volume ($\times 10^3$ kbar) compressibilities for AVO_3 materials.

	A: Compressibilities				B: Ratios	
	a	*b*	*c*	*V*	*a* : *c*	*b* : *c*
KVO_3	0	3.83	6.00	1.18	0	0.64
$RbVO_3$	9.20	8.12	5.69	2.33	1.62	1.43
$CsVO_3$	10.20	17.43	3.17	1.59	3.21	5.49
$RbVO_3$ (high P)	0.15	0.04	0.24	0.04		

3.1.2. Infrared data. The pressure dependence of the mid-infrared spectrum of KVO_3 is shown in figures 3 and 4 and table 2. Factor group analysis predicted nine bands in the mid-infrared region [2], seven due to V–O stretching and two to VO_2 bending. All these bands were observed under DAC conditions except for one VO_2 bending mode. All the observed bands shifted to a higher frequency with increasing pressure at rates close to those reported for the corresponding modes of $RbVO_3$.

In contrast to the EDXRPD results, only minor changes were observed in the infrared spectrum up to 48 kbar (the disappearance of one shoulder near 860 cm^{-1} and the appearance of another near 840 cm^{-1}). At 48 kbar there were significant changes: a band of moderate intensity appeared near 840 cm^{-1}; the bands originally at 698 and 494 cm^{-1} shifted discontinuously in frequency; those originally at 894 and 927 cm^{-1} merged, and a new weak band appeared at 650 cm^{-1}.

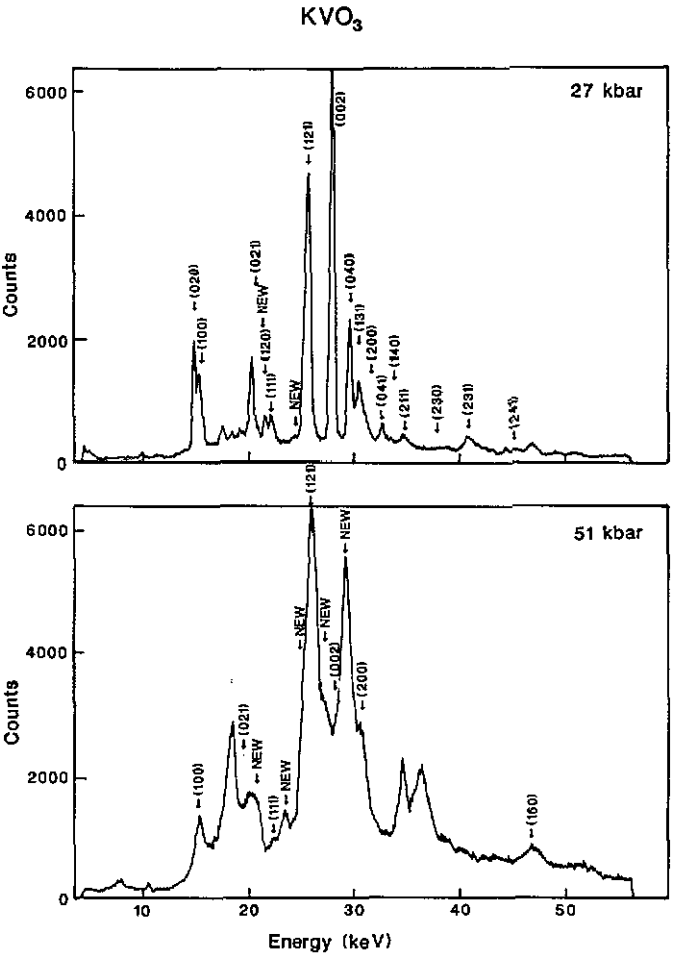

Figure 1. EDXRPD spectrum of KVO_3 at (*a*) 27 kbar, showing onset of phase transition, and (*b*) at 51 kbar.

Table 2. Infrared data (in cm^{-1}) for KVO_3 at high pressure (s = strong, m = medium, w = weak, sh = shoulder, br = broad).

Phase I (14 kbar) ν	$d\ln\nu/dP$ ($\times 10^4$ $kbar^{-1}$)	Phase II (69 kbar) ν
971 m	3.6	975 m
938 sh		
931 s	1.6	917 ms
899 m	4.2	
869 m	4.7	872 s
851 sh		835 sh
705 s, br	6.0	740 s, br
499 wm	1.2	474 w, br

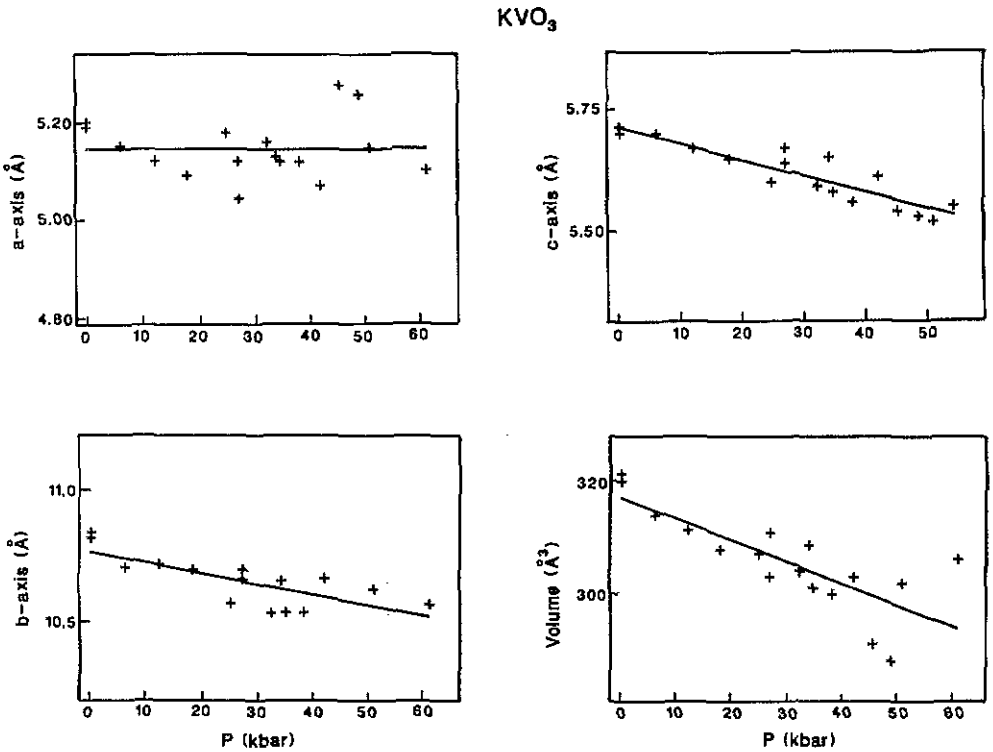

Figure 2. Variation with pressure of the lattice parameters of KVO_3.

3.1.3. Deductions. The x-ray and infrared data concur in showing that there is a phase transition in KVO_3. Whilst the major infrared changes occur near 48 kbar, there are subtle developments as low as 33 kbar. In the light of the x-ray results, these can be taken as supportive of the onset of a phase change. We conclude that there is a sluggish phase transition in KVO_3, beginning at 26 kbar and complete by 48 kbar.

3.2. $RbVO_3$

Plots of the refined orthorhombic cell parameters against pressure (figure 5) show sharp changes of slope near 40 kbar, indicative of a phase change. This is presumably the same structural reorganization reported at 53 kbar on the basis of the infrared study [2]. Although the discrepancy is disturbing, the explanation is probably that the x-ray data are more sensitive to the onset of a phase change than the infrared methods, as for KVO_3. No new diffraction lines were observed between 40 and 120 kbar, despite the clear breaks in slope of the lattice parameter plots. The absence of a volume discontinuity or peak splitting indicates that this is a second-order transition preserving the orthorhombic cell metric.

3.3. $CsVO_3$

In contrast with KVO_3, this material showed no change of diffraction pattern to 103 kbar. Unlike $RbVO_3$, the lattice parameters showed no change of slope with

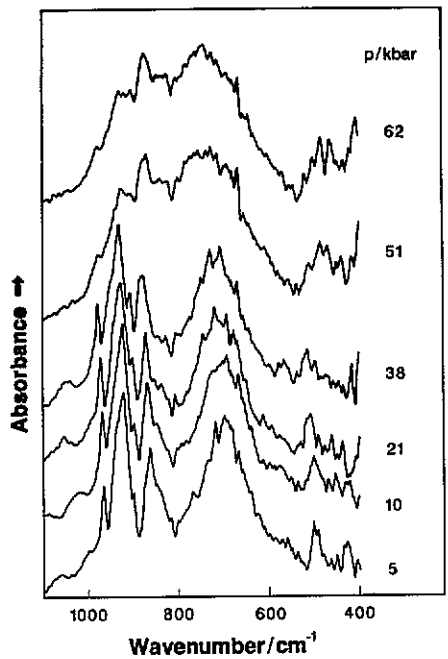

Figure 3. Evolution of the mid-infrared spectrum of KVO_3 with pressure.

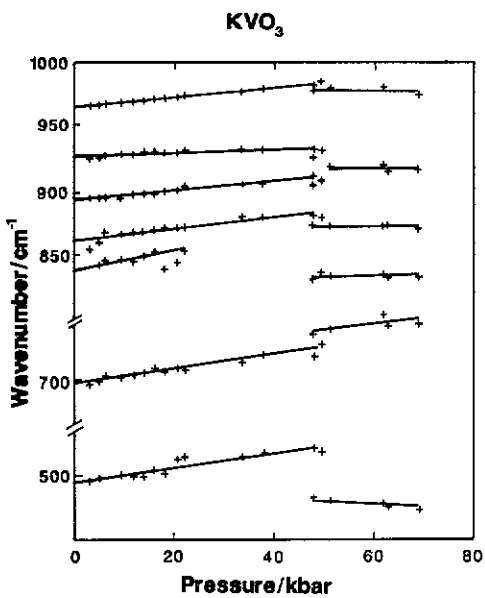

Figure 4. Pressure dependencies of the mid-infrared mode frequencies of KVO_3.

pressure (figure 6). We conclude that the parent orthorhombic phase remains stable to at least 100 kbar.

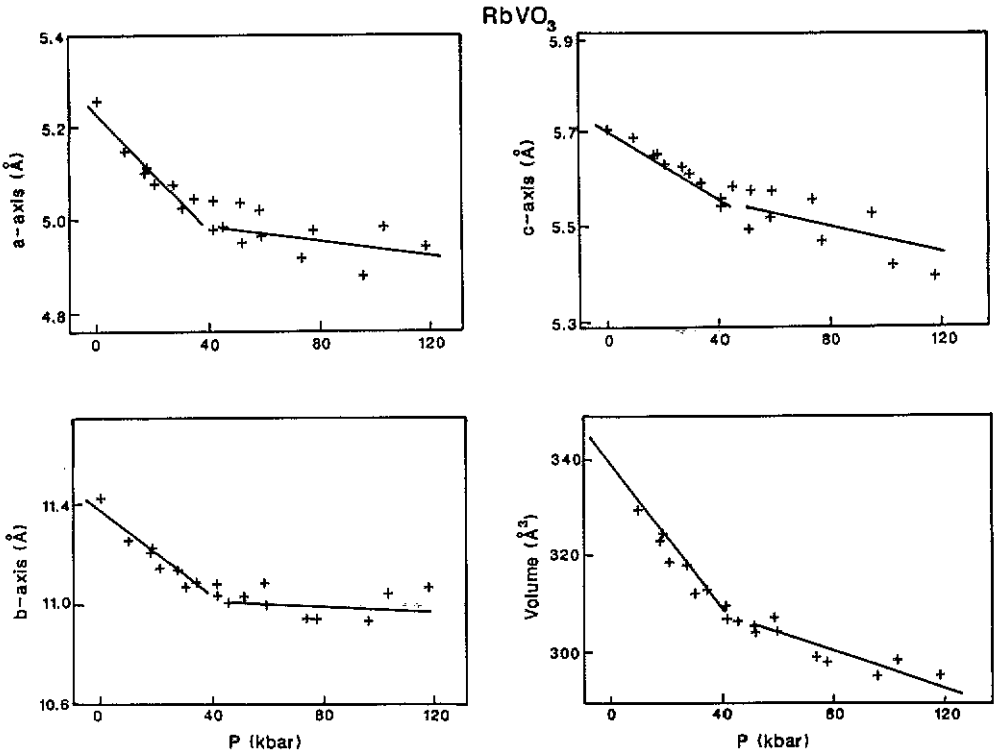

Figure 5. Variation with pressure of the lattice parameters of $RbVO_3$.

4. Discussion

In the orthorhombic (*Pbcm*) structure adopted by these materials, there are two vanadate chains per cell running parallel to *c*, with a $[V_2O_6]$ repeat. Since the bonding within each chain is highly directional and stronger than bonds to the A cations, it is reasonable to assume that these materials will be least compressible along *c*. Compression along the *a*- or *b*-axes will affect A to oxygen distances, which are expected to respond readily to stress. This is the pattern of behaviour shown by both the caesium salt, and by $RbVO_3$ up to the discontinuity at 40 kbar. Moreover, both the absolute values of compressibilities, and the ratios of uniaxial compressibilities along *a* or *b* relative to that along *c*, are larger in $CsVO_3$ than in $RbVO_3$. Thus far the results accord with expectation.

The behaviour of KVO_3 differs dramatically from that of the other materials in that the chain direction is the most compressible (table 1). This conflicts with the infrared evidence as both KVO_3 and $RbVO_3$ exhibit very similar mode frequency shifts with pressure, as expected since the bands in question are from internal modes of the vanadate chain and should not be greatly affected by change of A cation. Moreover, the changes in the spectrum at the transition in KVO_3 bear a close resemblance to those observed at the transition in $RbVO_3$, although quite different mechanisms are proposed later on the basis of the x-ray data. All that can be safely deduced from these results is that similar influences act upon the chain internal modes in each case, and that internal modes tell us relatively little about the overall structure.

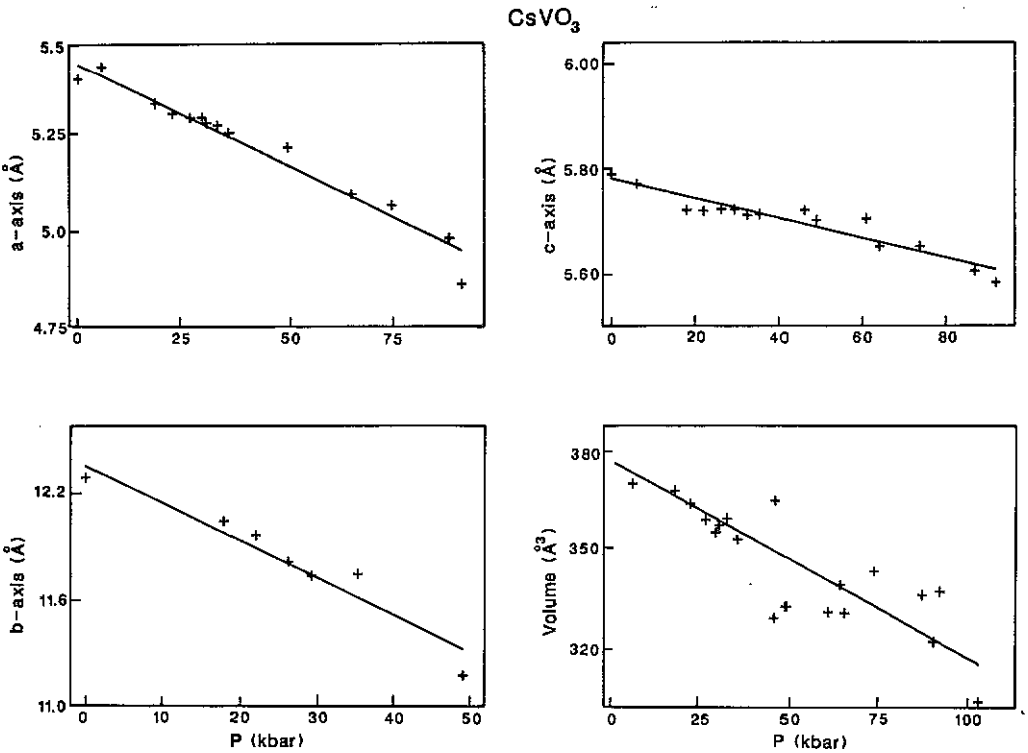

Figure 6. Variation with pressure of the lattice parameters for $CsVO_3$.

4.1. Models for the phase transitions

4.1.1. KVO_3. The data can be accommodated by a model in which the symmetry of the phase is reduced to monoclinic. The negligible compressibility along the *a*-axis suggests that the new cell is sheared on (100) relative to that of the parent orthorhombic structure. This shear would involve the vanadate chains slipping relative to each other along their lengths.

In this discussion, the monoclinic cell is maintained in its non-standard 'third setting' with *a* as the unique axis, and *b* and *c* approximately parallel to their equivalents in the orthorhombic phase. This is to facilitate comparison between these and other related structures later.

Taking unit cell edge lengths equal to those of the orthorhombic phase just below the transition, and an initial estimate of $\alpha = 99°$, 18 lines of the high-pressure EDXRPD pattern were successfully indexed (table 3).

The highest-symmetry subgroup of *Pbcm* with the requisite cell metric is $P2/b11$ ($P2/c$ in the second axial setting, more usual for monoclinic crystals). Adjacent chains are still related by the *b*-glides, and all the bridging oxygen atoms of the vanadate chains lie on diad axes. There is no unequivocal evidence for any further symmetry reduction such as loss of the centres of symmetry.

The unit cell of the proposed high-pressure structure is illustrated in figure 7.

4.1.2. $RbVO_3$. The EDXRPD patterns for the Rb salt indicate that the high-pressure

Table 3. *d*-spacings for KVO_3 at 51 kbar refined on a monoclinic cell. $a = 5.2703$ Å, $b = 9.8626$ Å, $c = 5.5231$ Å, $\alpha = 99.06°$, $V = 283.50$ Å^3. d_o is the observed value, d_c the calculated one.

h	k	l	d_o	d_c	$100(d_o - d_c)/d_c$
1	−1	0	5.0880	5.1146	0.5224
1	1	0	4.6801	4.6351	0.9605
0	1	1	4.4320	4.4682	0.8174
1	0	1	3.7358	3.7900	1.4504
1	1	−1	3.6700	3.6704	0.0096
1	2	−1	3.1164	3.1634	1.5091
0	3	−1	3.0200	3.0055	0.4801
1	3	0	2.7574	2.7641	0.2446
0	0	2	2.6818	2.7271	1.6888
1	3	−1	2.5760	2.6108	1.3509
0	4	0	2.4555	2.4349	0.8398
2	1	1	2.2662	2.2698	0.1590
1	4	0	2.2087	2.2104	0.0760
1	4	−1	2.1546	2.1588	0.1951
0	4	−2	1.9679	1.9776	0.4926
1	3	2	1.8246	1.8229	0.0910
3	0	1	1.6734	1.6722	0.0746
1	4	−3	1.5185	1.5144	0.2730

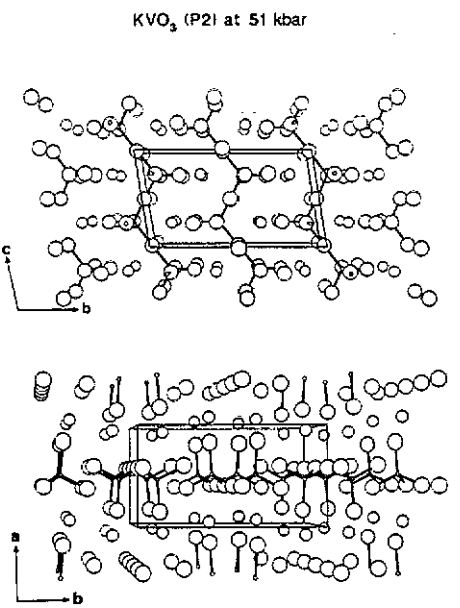

Figure 7. The structure of monoclinic KVO_3. The atoms are shown as spheres of relative sizes $K = 3, V = 1, O = 7$.

phase is metrically orthorhombic, with no discontinuity in cell parameters at the transition.

It was previously noted that $RbVO_3$ is most compressible along the *a*-axis, suggesting that a model for the 40 kbar phase change might include reorganization of

the unit cell in this direction. Shifting the two vanadate chains of the cell along a, so that they are no longer related to each other by centres of symmetry, results in a structure with the new space group $P2cm$. A displacive transition into this structure would affect only relative peak intensities in the powder pattern. In practice, this would probably not be observable due to the familiar problem of the unreliability of quantitative intensity information with the EDXRPD method.

The orthorhombic cell of $RbVO_3$ is shown in figure 8, with possible directions for chain motion.

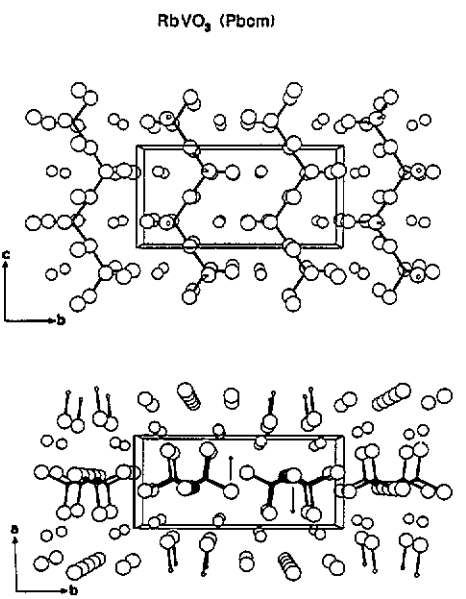

Figure 8. The structure of low-pressure orthorhombic $RbVO_3$, showing possible directions of chain motion to produce the high-pressure phase.

4.1.3. Comparison with silicate pyroxenes. One of the reasons for beginning this work was to compare the phase behaviour of the alkali-metal vanadates with that of the silicate pyroxenes, $A^{II}SiO_3$. Both groups of materials contain chains of tetrahedrally coordinated cations (V or Si), there being a two-tetrahedron repeat in each case. The vanadate structures are simply related to those of the silicate pyroxenes by a $b/2$ translation of (100) structural slabs. This increases the coordination number of the A cation from 6–8 to 8–10 [1].

The silicate pyroxenes display a simple pattern of crystal chemically controlled polymorphism in which the structures adopted and their stability ranges in terms of pressure and temperature are highly cation-dependent. This is precisely what we have discovered in the alkali-metal vanadates, but with this remarkable difference: that, whereas the vanadates have the same structure under ambient conditions but diverge at pressure, the silicates do the opposite. Silicate pyroxenes have structures at 1 atm which strongly reflect A^{II} cation coordination requirements ($A^{II} \equiv$ Ca, Fe, Mg), but converge at high pressure to similar monoclinic structures. Furthermore, the atomic displacements involved in our models for the vanadate transitions are different from those operative in the silicate transitions.

The reason for this behavioural dichotomy must be related to the quite different Coulomb forces which help to stabilize the coordination arrangements around the singly charged cations in the vanadates or the doubly charged cations in the silicates.

5. Conclusions

A sluggish phase transition has been located in KVO_3, starting at 27 kbar and complete at 48 kbar. The changes in the powder pattern are consistent with monoclinic symmetry for the high-pressure phase. A structural model is proposed for this transition, involving slip of the vanadate chains relative to one another on (100).

$RbVO_3$ also shows a phase change (at 40 kbar) but this is not accompanied by a change in the EDXRPD pattern: these facts are consistent with a model involving slip of the chains in the a-direction, maintaining orthorhombic symmetry.

$CsVO_3$ shows no phase change to 103 kbar, and has uniaxial compressibilities in accord with expectations.

Acknowledgments

We thank the NSERC, Canada, for a fellowship to JH, and the SERC for a maintenance grant to SL and for other support.

References

[1] Hawthorne F C and Calvo C 1977 *J. Solid State Chem.* **22** 157
[2] Adams D M and Fletcher P A 1988 *Spectrochim. Acta* A **44** 233
[3] Klug D D and Whalley E 1983 *Rev. Sci. Instrum.* **54** 1205